Journal of Clinical and Translational Hepatology **2022** vol. 10(4) | 608–619
DOI: 10.14218/JCTH.2021.00301

Original Article

Extracellular Polysaccharide from *Rhizopus nigricans* Inhibits Hepatocellular Carcinoma via miR-494-3p/TRIM36 Axis and Cyclin E Ubiquitination

Haixiong Yan, XiaoQian Ma, Ze Mi, Zhenhu He and Pengfei Rong*

Department of Radiology, The Third Xiangya Hospital of Central South University, Changsha, Hunan, China

Received: 21 July 2021 | **Revised:** 11 October 2021 | **Accepted:** 27 October 2021 | **Published:** 21 February 2022

Abstract

Background and Aims: This study was designed to uncover the mechanism for extracellular polysaccharide (EPS1-1)-mediated effects on hepatocellular carcinoma (HCC) development. ***Methods:*** HCC cells were treated with EPS1-1, miR-494-3p mimic, sh-TRIM36, and pcDNA3.1-TRIM36. The levels of miR-494-3p and TRIM36 were measured in normal hepatocytes, THLE-2, and HepG2 and HuH7HCC cell lines, along with the protein expression of cyclin D/E and p21. The proliferation, cell cycle, and apoptosis of HCC cells were assayed. The interactions between miR-494-3p and TRIM36, and between TRIM36 and cyclin E were assessed. Finally, the expression and localization of TRIM36 and cyclin E were monitored, and tumor apoptosis was detected, in tumor xenograft model. ***Results:*** EPS1-1 suppressed HCC cell proliferation and cyclin D/E expression and promoted apoptosis and p21 expression. miR-494-3p was upregulated and TRIM36 was downregulated in HCC cells. Transfection with miR-494-3p mimic or sh-TRIM36 facilitated HCC cell proliferation and the expression of cyclin D/E protein but they inhibited apoptosis and p21 expression in the presence of EPS1-1. Overexpression of TRIM36 further consolidated EPS1-1-mediated inhibition of HCC proliferation, cyclin D/E, and the promotion of apoptosis and p21 expression. Those effects were reversed by miR-494-3p overexpression. TRIM36 was a target gene of miR-494-3p, and TRIM36 induced cyclin E ubiquitination. EPS1-1 suppressed cyclin E expression, promoted TRIM36 expression and tumor apoptosis, all of which were abrogated by increasing the expression of miR-494-3p *in vivo*. ***Conclusions:*** EPS1-1 protected against HCC by limiting its proliferation and survival through the miR-494-3p/TRIM36 axis and by inducing cyclin E ubiquitination.

Citation of this article: Yan H, Ma XQ, Mi Z, He Z, Rong P. Extracellular Polysaccharide from *Rhizopus nigricans* Inhibits Hepatocellular Carcinoma via miR-494-3p/TRIM36 Axis and Cyclin E Ubiquitination. J Clin Transl Hepatol 2022;10(4):608–619. doi: 10.14218/JCTH.2021.00301.

Introduction

Hepatocellular carcinoma (HCC) is the third leading cause of cancer-related death and remains one of the most aggressive malignancies worldwide.[1,2] Although liver resection is one of the most effective treatment options, the prognosis of HCC is extremely poor, with a 1-year survival of 40%.[3,4] Thus, identifying the underlying mechanisms contributing to the progression of HCC is crucial to facilitate the development of novel diagnostic biomarkers and effective therapeutic targets.

In recent years, considerable attention has been paid to the study of natural antitumor compounds with known biological activities and few or no side effects.[5,6] *Rhizopus nigrum*, a zygote filamentous fungus, has been extensively used by the pharmaceutical industry for production of organic acids and biotransformation.[7] An extracellular polysaccharide (EPS1-1) extracted from *R. nigricans* was found to exert antitumor activity and improve the immune response.[8–10] EPS1-1 was reported to not only suppresses colitis-related colorectal cancer[11] but also to have a role in ameliorating functional disorders of colorectal cancer in mice.[12] The involvement of EPS1-1 in biological processes including proliferation, metastasis, and apoptosis of colorectal cancer has been described.[13,14] Previous studies have indicated that EPS1-1 repressed the progression of HCC *in vitro* and *in vivo*,[15] but whether EPS1-1 can regulate biological processes and molecular mechanisms of HCC remains unclear.

Micro (mi)RNAs are small noncoding RNAs that post-transcriptionally regulate gene expression by degrading their target messenger (m)RNAs or by terminating translation. miRNAs are aberrantly expressed in a majority of human cancers, suggesting that they have essential roles in tumorigenesis and tumor development.[16] Moreover, miRNAs were reported to be involved in cellular processes including cell proliferation, apoptosis, and differentiation.[17] Up until now, a growing number of studies have elucidated the role of miRNA in the molecular pathogenesis of HCC. For example, abundant expression of miR-517a was associated

Keywords: Extracellular polysaccharide; EPS1-1; miR-494-3p; TRIM36; Ubiquitination; Hepatocellular carcinoma.

Abbreviations: CO-IP, co-immunoprecipitation; EPS1-1, extracellular polysaccharide; HCC, hepatocellular carcinoma; IHC, immunohistochemistry; miRNA, microRNA; MTT, methylthiazol tetrazolium; MUT, mutant type; NC, negative control; PI, propidium iodide; qRT-PCR, quantitative RT-PCR; SDS-PAGE, sodium dodecyl sulfate-polyacrylamide agarose gel electrophoresis; WT, wild type.

***Correspondence to:** Pengfei Rong, Department of Radiology, The Third Xiangya Hospital of Central South University, No. 138, Tongzipo Road, Yuelu District, Changsha, Hunan 410013, China. ORCID: https://orcid.org/0000-0001-5473-1982. Tel: +86-18684706350, Fax: +86-731-88618411, E-mail: rongpengfei66@163.com

with adverse outcomes in patients with HCC.[18] In contrast, miR-199a/b-3p and miR-219-5p were found to act as tumor suppressors in HCC.[19,20] Therefore, the identification of drug agents that substantially regulate oncogenic or tumor-suppressive miRNA expression may be a promising therapeutic strategy to treat or prevent human cancers. Previous studies have shown that miR-494-3p acts as an oncogene by stimulating the proliferation and invasion and suppressing apoptosis in glioma cells.[21] Also, increased miR-494-3p expression has been linked to HCC progression.[22] However, whether EPS1-1 can downregulate miRNAs, specifically miR-494-3p in HCC, remains unknown.

Our study investigated the potential involvement of EPS1-1 in the proliferation and apoptosis of HCC *in vitro* and its effect on tumor-bearing mice *in vivo*. Collectively, the findings demonstrate novel inhibitory effects of EPS1-1 on HCC development through modulation of the miR-494-3p/TRIM36 axis and ubiquitination of cyclin E.

Methods

Clinical sample

HCC and adjacent normal tissues were collected from 22 patients diagnosed at our hospital between October 2019 and December 2020. The tissues were preserved in liquid nitrogen for subsequent examination. All procedures involving humans were performed with the approval of the ethics committee of the Third Xiangya Hospital of Central South University and the informed consent of the patients or their relatives.

Cell culture

THLE-2 normal human hepatocytes and HepG2 and HuH7 HCC cell lines were acquired from the Cell Bank of Chinese Academy of Sciences (Shanghai, China). Exopolysaccharide EPS1-1 was purified from the fermentation broth of *R. nigricans*. HepG2 and HuH7 cells were cultured in Dulbecco's Modified Eagle Medium (DMEM) supplemented with 10% fetal bovine serum (ThermoFisher Scientific, Waltham, MA, USA) at 37°C in a 5% CO_2 incubator. The cells at approximately 90% confluency were dissociated with 0.25% trypsin followed by addition of serum-containing medium to terminate digestion. The cells were then gently pipetted into single-cell suspension and passaged.

Transient transfection

HepG2 and HuH7 cells were inoculated onto 96-well plates at a density of 1×10^4 cells/well. When the adherent cells reached 60% confluency, miR-494-3p inhibitor/mimic (100 nmol) plasmids containing silenced (sh-TRIM36, 2 μg) or overexpressed (oe-TRIM36, 2 μg) TRIM36, inhibitor/mimic negative control (NC) or sh-NC/oe-NC (Shanghai GenePharma Co., Ltd., Shanghai, China) was transfected into the cells with Lipofectamine 2000 (ThermoFisher Scientific) following the manufacturer's instructions. Subsequent experiments were carried out 48–72 h later.

Cell grouping

Cells were allocated to be treated for 72 h with EPS1-1 25 μg/mL, 50 μg/mL, 100 μg/mL, or 200 μg/mL. After transfection, HCC cells were treated 200 μg/mL of EPS1-1 for 24 h and then divided into EPS1-1, EPS1-1 + mimic NC, EPS1-1 + miR-494-3p mimic, EPS1-1 + sh-NC, EPS1-1 + sh-TRIM36, EPS1-1 + oe-NC, EPS1-1 + oe-TRIM36 group, and EPS1-1 + oe-TRIM36 + miR-494-3p mimic groups. After transfection with pcDNA3.1 or pcDNA3.1-TRIM36, HCC cells were induced with 20 μM protease inhibitor MG132 for 4 h and divided into oe-NC + DMSO, oe-TRIM36 + DMSO, oe-NC + MG132, and oe-TRIM36 + MG132 groups.

Methylthiazol tetrazolium (MTT) assay

Cells at a density of 5×10^3 cells/well were plated onto 96-well plates. At indicated time points (24, 48, or 72 h), 10 μl of MTT solution (5 mg/mL) was added to each well at 37°C for 4 h. Subsequently, 100 μL DMSO was added and the cells were incubated overnight at 37°C to terminate the reaction. The absorbance (optical density, OD) was recorded at a wavelength of 490 nm using a microplate reader (Sectramax 190, Molecular Devices Corp., Sunnyvale, CA, USA). The OD value represents cell viability. The results from three independent assays of each group were calculated and averaged. A proliferation curve was plotted for optimum visualization of the viability data.

Flow cytometry

For the detection of cell apoptosis, single-cell suspensions of cells in each group were prepared and centrifuged at 2,000 rpm. After washing twice with phosphate buffered saline (PBS), the cells were resuspended in binding buffer. Then, 5 μL of Annexin-V-FITC and propidium iodide (PI) were added to 195 μL cell suspension containing 10^5 cells and cultured for 10 min in the dark. Cell apoptosis was assayed by flow cytometry (BD FACS Canto II, 488N, San Jose, CA, USA).

For analysis of cell cycle events, cells from each group were seeded onto 6-well culture plates (3×10^5 cells/well) for 24 h. Cells were then fixed with 4% paraformaldehyde (Shanghai Sangon Biological Engineering Co., Ltd., Shanghai, China) for 15 min before incubation with 50 μg/mL PI (Solarbio, Beijing, China) in the dark (37°C, 30 min). The fluorescence intensity of cells (excitation wavelength 488 nm) was assessed by flow cytometry (BD FACS Canto II, 488N, San Jose, CA, USA)

Quantitative RT-PCR (qRT-PCR)

Total RNA was extracted using TRIzol reagent (Thermo Fisher Scientific, MA, USA) following the manufacturer's instructions. The extracted RNA was reverse transcribed into cDNA using a reverse transcription system (Promega, Madison, WI, USA). Gene expression was detected using a LightCycler 480 qRT-PCR instrument (Roche, IN, USA), and reactions were performed with a qRT-PCR kit (SYBR Green PCR kit, Takara Bio, Inc., Otsu, Japan). Thermal cycling conditions were: initial denaturation 5 min at 95°C, and 40 cycles of denaturation for 10 s at 95°C, annealing 10 s at 60°C, and elongation 20 s at 72°C. miR-494-3p and TRIM36 expression were normalized against U6 and GAPDH, respectively. Data were analyzed by the $2^{-\Delta\Delta Ct}$ method. The primer sequences are shown in Table 1.

Western blotting

Cells were lysed in RIPA buffer containing Halt protease

Table 1. Primer sequences for qRT-PCR assays

Primer	Sequence
miR-494-3p-F	CTCCAAAGGGCACATA
miR-494-3p-R	GCAGGGTCCGAGGTATTC
U6-F	GCTTGCTTCGGCAGCACATATAC
U6-R	TGCATGTCATCCTTGCTCAGGG
TRIM36-F	CTGCACTGAAACCAGCTCTTG
TRIM36-R	ACTAGCTCTGCTCACCCAAA
Cyclin E-F	CAACAAACACAGGGGGCAAC
Cyclin E-R	AGCTGTTTTTCGACCACCCA
GAPGH-F	GTCAGTGGTGGACCTGACCT
GAPDH-R	TGCTGTAGCCAAATTCGTTG

F, forward; R, reverse.

inhibitor cocktail (Pierce, Rockford, IL, USA) and phosphatase inhibitors (Cayman Chemical, Ann Arbor, MI, USA), and the protein concentration was determined by the Bradford method. Sodium dodecyl sulfate-polyacrylamide agarose gel electrophoresis (SDS-PAGE) was run at 120 V for protein separation. Thereafter, the proteins were transferred from the gel to polyvinylidene fluoride (PVDF) membranes and blocked in TBS-Tween (TBS-T) supplemented with 0.05 g/mL bovine serum albumin for 1 h. The membranes were then incubated with primary antibodies against GAPDH (1:10,000, ab181602), TRIM36 (1:1,000, ab272672), and cyclin E (1:1,000, ab33911) (Abcam, Cambridge, MA, USA) overnight at 4°C. After washing with TBS-T, the membranes were incubated with goat anti-rabbit IgG (1:5,000, Beijing ComWin Biotech Co., Ltd., Beijing, China) for 2 h at room temperature, followed by washing three times in TBS-T. Protein bands were quantified by chemiluminescence imaging analysis system (GE Healthcare, Beijing, China) using an electrogenerated chemiluminescence (ECL) reagent.

Dual luciferase reporter assay

Starbase database was used to predict the binding site between miR-494-3p and TRIM36, and TRIM36-3′UTR wild sequence and mutated TRIM36-3′UTR sequence were synthesized. These two sequences were cloned into dual luciferase reporter vector (pGL3-Basic) to construct the wild dual luciferase reporter (WT-TRIM36) and the mutant dual luciferase reporter (MUT-TRIM36) carrying the 3′UTR of TRIM36. HepG2 and HuH7 cells (5×10^5/well) were seeded into 6-well plates and maintained in a humidified 5% CO_2 incubator for 24 h at 37°C. Thereafter, the cells were co-transfected with a pGL3-TRIM36-3′ UTR luciferase reporter vector and 5 μL of miR-494-3p mimic or its normal control (NC) for 6 h at 37°C using Lipofectamine 2000 following the manufacturer's recommendations.Dual luciferase reporter assay system was used to detect the activity.

Co-immunoprecipitation (CO-IP)

Whole-cell lysates were centrifuged and incubated with 2 μg of anti-TRIM36 (sc-100881, Santa Cruz Biotechnology, Santa Cruz, CA, USA), anti-cyclin E (ab33911, Abcam, Cambridge, MA, USA) or normal IgG antibodies and protein G-Agarose beads (Roche Diagnostics Ltd, Shanghai, China) overnight at 4°C. The immunocomplexes were separated by SDS-PAGE and then blotted with the indicated antibodies.

Ubiquitination assay

Oe-TRIM36 or oe-NC were transfected into HepG2 cells, after which the lysates were immunoprecipitated with IgG (ab172730) or anti-cyclin E (ab33911, Abcam, Cambridge, MA, USA) antibody at 4°C overnight. Bound proteins that eluted from the protein G-Agarose beads were separated by SDS-PAGE and then immunoblotted with an anti-Ub antibody (ab134953, Abcam, Cambridge, MA, USA).

Animals

Pathogen-free (SPF) BALB/c male nude mice 4–5 weeks of age and weighing 14–18 g were obtained from Vital River Lab Animal Technology Co, Ltd (Beijing, China). The mice were bred under SPF conditions at the Third Xiangya Hospital of Central South University and kept at 26–28°C, 40–60% humidity, a 10 h light period, and water and food ad libitum for 1 week before use. All animal studies were performed following animal experimentation protocols approved by the Third Xiangya Hospital of Central South University, and care was taken to minimize pain to the animals.

Tumor xenograft experiments

The experiments were done in compliance with the ethics committee of the Third Xiangya Hospital of Central South University. Twenty-four male BALB/C nude mice (Vital River, Beijing, China) weighing 14–18 g and 4–5 weeks of age were divided into control, EPS1-1, EPS1-1 + mimic NC, and EPS1-1 + miR-494-3p mimic groups of six mice each. HepG2 cells transfected with mimic NC or miR-494-3p mimic were maintained in DMEM (200 μg/mL) for 24 h. Stably transfected cells then were selected, identified, and cultured. The cells were dissociated with trypsin and gently pipetted to form single-cell suspensions. The cell density was adjusted to 10^5 cells/mL. Mice were subcutaneously injected with 0.2 mL of the single-cell suspension and observed regularly to record the body weight and tumor length and width. The tumor size and volume were calculated weekly by detecting the luciferase activity of tumors using a real-time imaging system. After 28 days, the nude mice were sacrificed to obtain the tumors. The tumor weights and volumes were determined.

Immunohistochemistry (IHC)

Sections were heated for 4 h in an oven at 65°C, after which the sections were dewaxed in xylene and ethanol. Thereafter, the sections were placed into a citrate antigen retrieval solution before being boiled in a pressure cooker, cooled to room temperature, and washed three times for 3 m in PBS before adding 3% peroxidase inhibitor for 10 min and washing again three times in PBS. A non-specific staining blocker was added for 15 min at room temperature. PBS-diluted primary antibodies against TRIM36 (1:100, sc-100881, Santa Cruz Biotechnology, Santa Cruz, CA, USA) and cyclin E (1:100, ab135380, Abcam, Cambridge, MA, USA) were added to the slides for incubation overnight at 4°C in a refrigerator. The next day, the sections were taken from the refrigerator and rewarmed for 1 h to room temperature to remove excess primary antibodies, followed by PBS wash-

ing (3 × 3 m). The sections were incubated with secondary antibody (1:1,000, ab6728, Abcam, Cambridge, MA, USA) for 30 min at room temperature before washing with PBS (3 × 3 m). A few drops of streptavidin-H_2O_2 were added to the sections and incubated for 15 min at room temperature, after which the sections were washed with PBS (3 × 3 m). The sections were then stained with hematoxylin for 2 min, washed with tap water for 10 min, differentiated in 2% hydrochloric acid alcohol for 15 s, and washed with tap water (10 min). Following dehydration in ethanol, permeabilization with xylene, and mounting, the sections were observed by light microscopy and photographed.

TUNEL assay

Tumor sections were fixed 30 m in 0.5 mL 4% paraformaldehyde for 30 m. The paraformaldehyde was removed, the sections were washed once in 0.5 mL of PBS, and then permeabilized by 0.5 mL of Triton X-100 for 5 min. The permeabilization solution was discarded and the sections were washed twice in 0.5 mL PBS, each for 5 min. TUNEL reaction mixture (5 μL TdT plus 45 μL dUTP label) was added and incubated in the dark at room temperature for 1 h. The mixture was removed and the sections were washed three times in 0.5 mL PBS. After the PBS was discarded, DAPI was used for nuclear staining.

Immunofluorescence

Tumor sections were baked in a 60°C incubator for 60–90 m and immersed in xylene for 10 m. Thereafter, the xylene was replaced and the sections were maintained in xylene for another 10 m. The sections were successively placed for 5 m in absolute, 95%, 85%, 75% ethanol, and distilled water followed by washing three times in PBS. Then, antigen retrieval was performed (0.01 M citrate buffer solution, pH 6.0; boiling in microwave oven and heating over low heat for 16 min), and the sections were washed three times for 5 m in PBS and blocked in 5% goat serum for 30 min at room temperature. Excess serum was removed and the sections were incubated at 4°C overnight with 50 μL of primary antibody against TRIM36 (1:100, ab272672) or cyclin E (1:100, ab33911) in a wet bot, with PBS as a negative control. After incubation, the sections were rewarmed to 37°C for 30–45 min and washed three times in PBS for 5 min. The sections were wiped dry, and multi-fluorescein-labeled homogenous secondary antibody (40–50 μL) was added for incubation 50 m at room temperature in the dark. After washing three times in PBS for 5 min, the sections were counterstained, and nuclei were stained for. 5 min with DAPI 5 μg/mL. The sections were rinsed four times for 5 min, and 30 μL of antifade reagent was added before coverslips were added. The tissue was observed by fluorescence microscopy (Leica, Germany).

Statistical analysis

All experiments were conducted in triplicate except as otherwise noted, and the data were reported as means ± standard deviation. The statistical analysis as performed with SPSS 18.0 (IBM Corp., Armonk, NY, USA) and GraphPad Prism 6.0 (GraphPad Software Inc., San Diego, CA, USA). Between-group comparisons were performed by *t*-tests, and one-way analysis of variance was used for multiple-group comparisons followed by the Dunnett's multiple comparisons test. *P*-values <0.05 were considered statistically significant.

Results

EPS1-1 suppresses HCC cell proliferation and promotes apoptosis

The effects of EPS1-1 on HCC cells were investigated *in vitro* by assays of cell proliferation in cultures treated with concentrations from 25 to 200 μg/mL. EPS1-1 effectively reduced the proliferation of HepG2 and HuH7 HCC cells in time- and dose-dependent manners (Fig. 1A). Flow cytometry showed that EPS1-1 treatment resulted in a dose-dependent G0/G1 phase arrest in HepG2 and HuH7 cells (Fig. 1B), indicating that EPS1-1 inhibited the growth of HCC cells. The expression of the cell cycle regulatory proteins cyclin D/E and cyclin-dependent kinase inhibitor (CDKI) p21 was assessed by SDS-PAGE. EPS1-1 treatment significantly repressed cyclin D and cyclin E expression and enhanced p21 expression in a dose-dependent manner (Fig. 1C), corroborating the MTT and flow cytometry results that demonstrated the inhibition of HCC cell proliferation by EPS1-1. Annexin V-FITC/PI staining and flow cytometry found that compared with the control (0 μg/mL), cell apoptosis significantly increased after treatment with 100 μg/mL and 200 μg/mL EPS1-1 (Fig. 1D). The overall findings indicate that EPS1-1 inhibited the proliferation and stimulated the apoptosis of HCC cells *in vitro*.

EPS1-1 hinders HCC progression by inhibiting miR-494-3p

miR-494-3p expression was greater in HepG2 and HuH7 HCC cells than it was in THLE-2 cells (Fig. 2A), and miR-494-3p expression was consistently found to be higher in cancer tissue collected from HCC patients compared with noncancerous, normal tissue collected from the patients (Fig. 2B). To evaluate the correlation of miR-494-3p expression with clinicopathological features, the patients were divided into groups with high or low miR-494-3p expression based on the mean value of miR-494-3p expression. As shown in Table 2, miR-494-3p was correlated with tumor size, tumor number and tumor, node, and metastasis (TNM) stage, but was not correlated with gender and age. To investigate the relationship of EPS1-1 treatment with miR-494-3p expression, miR-494-3p transcript levels were monitored in HCC cells after treatment with different doses of EPS1-1. miR-494-3p expression was significantly suppressed after EPS1-1 (100 μg/mL and 200 μg/mL) treatment compared with the control (0 μg/mL) (Fig. 2C). The data implied that EPS1-1 inhibited HCC cell proliferation and facilitated apoptosis by downregulating miR-494-3p expression. As 200 μg/mL EPS1-1 exhibited the most potent suppression of miR-494-3p in HCC cells compared with the control (Fig. 2C), that concentration was used in subsequent procedures.

The involvement of miR-494-3p in EPS1-1-modulated proliferation and apoptosis was confirmed in transfected HCC that overexpressed miR-494-3p. The transfection efficiency of the miR-494-3p mimic in HepG2 and HuH7 cells were assessed by qRT-PCR, which showed significantly enhanced miR-494-3p expression in HepG2 and HuH7 cells (Fig. 2D). The proliferation of HCC cells in the control, EPS1-1, EPS1-1 + mimic NC, and the EPS1-1 + miR-494-3p mimic groups showed that EPS1-1 treatment led to decreased HCC proliferation, but that the decrease was not sustained when miR-494-3p mimic was overexpressed in the EPS1-1 + miR-494-3p mimic group (Fig. 2E). Flow cytometry revealed that EPS1-1 treatment led to an increase in the percentage of cells in the G0/G1 phase compared with its control, but that was not observed in cells transfected with the miR-494-3p mimic (Fig. 2F**)**. To further study the effects on the cell cycle,

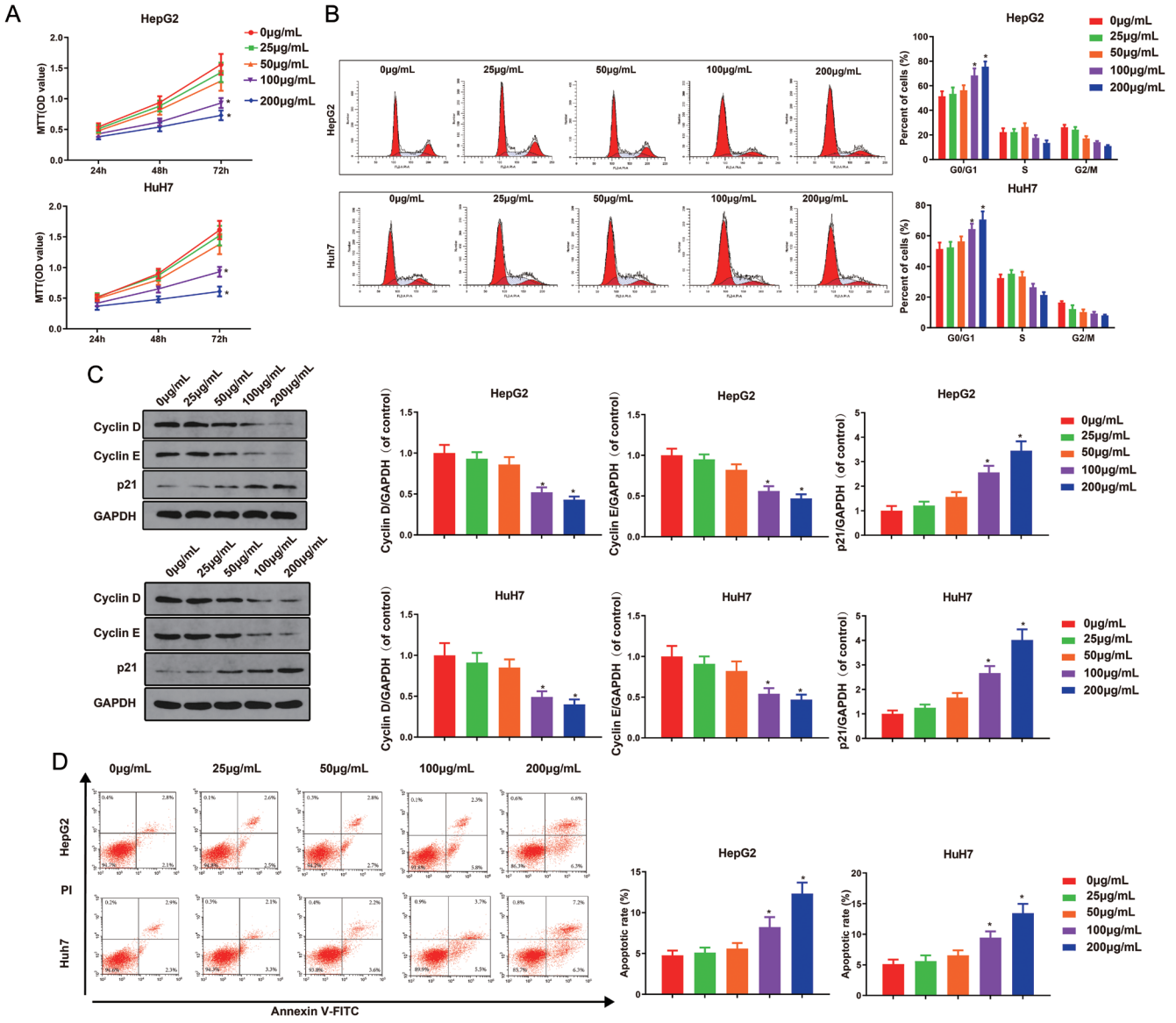

Fig. 1. EPS1-1 inhibits HCC cell proliferation and facilitates apoptosis. MTT assay of cell proliferation (A). Flow cytometry assay of the cell cycle (B). Western blot assay of the cell cycle regulatory proteins cyclin D, cyclin E, and p21 (C). Annexin V-FITC/PI staining assay of cell apoptosis (D). *p<0.05 vs. control. Data are means ± standard deviation; independent-sample t-test or one-way analysis of variance and Tukey's. Each assay was performed in triplicate. FCM, flow cytometry; HCC, hepatocellular carcinoma; PI, propidium iodide.

cyclin D and E, and p21 expression were assayed in western blots. Cyclin D and cyclin E expression were repressed and p21 expression was upregulated, and in spite of EPE1-1 treatment, the expression patterns were reversed when the miR-494-3p mimic was overexpressed (Fig. 2G). Annexin V-FITC/PI staining showed that EPS1-1 treatment increased apoptosis in HCC cells and that apoptosis decreased in the EPS1-1 + miR-494-3p mimic group (Fig. 2H) compared with control. Overall, the findings showed that EPS1-1 inhibited HCC cell proliferation and promoted apoptosis by suppressing miR-494-3p expression.

TRIM36 is a target gene of miR-494-3p

To understand the mechanism of miR-494-3p-mediated HCC progression further, we screened for its targets, which led us to examine an E3 ubiquitin ligase TRIM36 expression in THLE-2 normal hepatocyte cells, and HCC cell lines. Reportedly, TRIM36 was downregulated in gastric cancer and prostate cancer, but little is known with regard to its function in the HCC. TRIM36 was weakly expressed at both transcript and protein levels in HepG2 and HuH7 cells in contrast to THLE-2 cells (Fig. 3A), and TRIM36 expression was downregulated in tissues collected from the HCC group patients compared with adjacent normal tissue (Fig. 3B). As shown in Figure 3C, StarBase, a database of known microRNA–mRNA interactions, indicated that miR-494-3p could bind to the 3′-UTR of TRIM36. The direct interaction between miR-494-3p and TRIM36 was confirmed with a dual luciferase reporter carrying the 3′-UTR of TRIM36, which showed that transfection of miR-494-3p mimic significantly

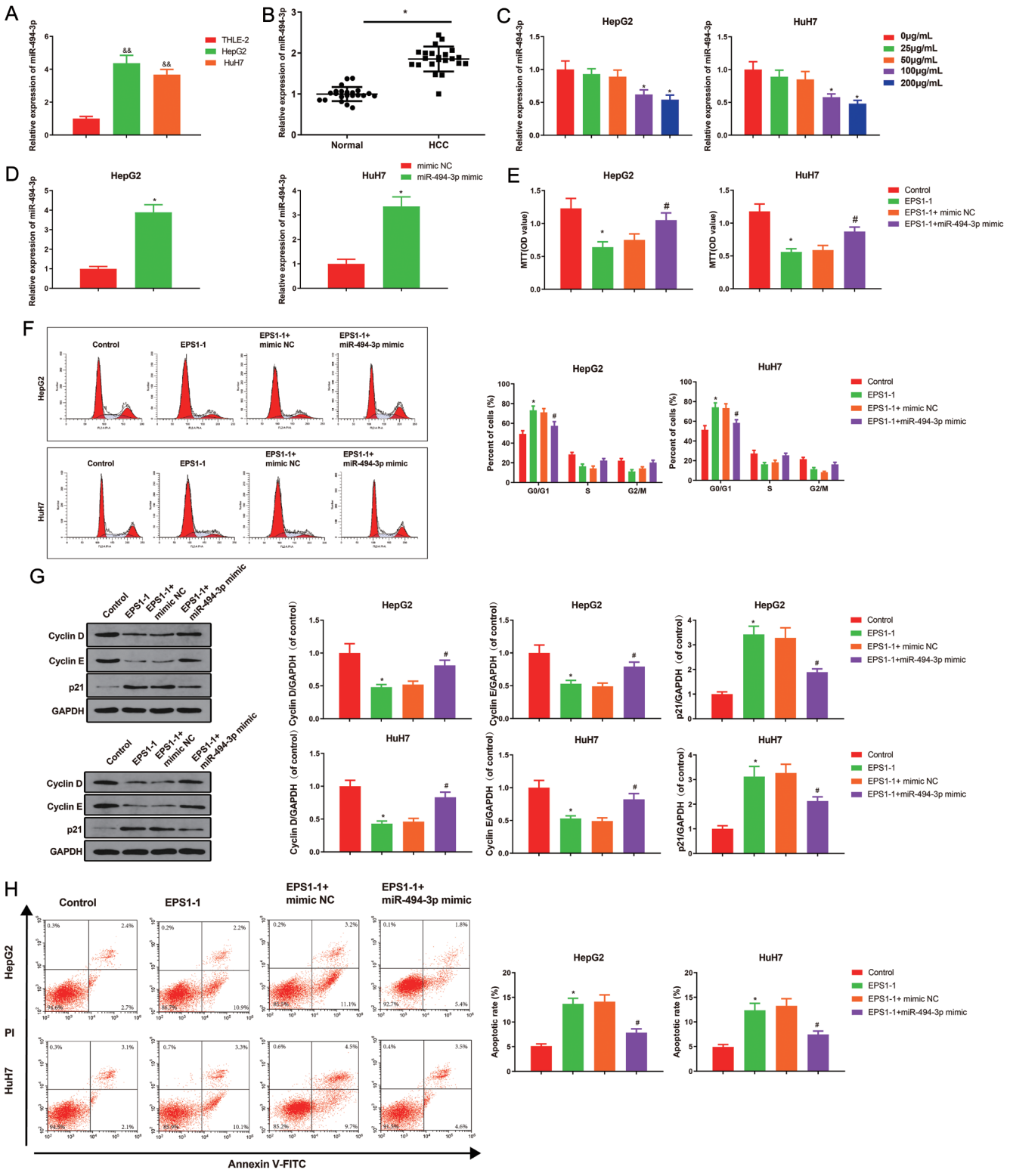

Fig. 2. EPS1-1 inhibits HCC progression via inhibiting miR-494-3p. miR-494-3p is strongly expressed in HepG2 and HuH7 HCC cells (A). miR-494-3p expression was increased in HCC tissues (B). EPS1-1 repressed miR-494-3p expression in HCC cells (C). qRT-PCR assay of the transfection efficiency of the miR-494-3p mimic (D). MTT assay of HCC cell proliferation (E). Flow cytometry assay of the HCC cell cycle in each study group were monitored by FCM (F). Western blot assays of the cell cycle regulatory proteins cyclin D, cyclin E, and p21 (G). Annexin V-FITC/PI staining assay of cell apoptosis (H). *$p<0.05$, **$p<0.01$ vs. control, mimic NC group or normal group. $^{\&\&}p<0.01$ vs. THLE-2, $^{\#}p<0.05$ vs. EPS1-1 + mimic NC. Data are means ± standard deviation; independent-sample *t*-test or one-way analysis of variance and Tukey's. Each assay was performed in triplicate. FCM, flow cytometry; HCC, hepatocellular carcinoma; PI, propidium iodide.

Table 2. Correlation of miR-494-3p with the clinicopathological features of patients with hepatocellular carcinoma

Clinicopathological factor	Low miR-494-3p (*n* = 11)	High miR-494-3p (*n* = 11)	*p*-value
Sex			
Male, *n*	5	7	0.6699
Female, *n*	6	4	
Age, years			
≤55	6	6	1
>55	5	5	
Tumor size, cm			
≥5	1	9	0.0019**
<5	10	2	
Tumor number			
Multiple	2	8	0.0300*
Single	9	3	
TNM stage			
I-II	8	2	0.0300*
III-IV	3	9	

suppressed the luciferase activity of wild-type (WT)-TRIM36 ($p<0.01$) and that the luciferase activity of mutant (MUT)-TRIM36 was unaffected (Fig. 3D). In addition, qRT-PCR and western blotting confirmed that transfection of the miR-494-3p mimic significantly decreased TRIM36 expression and that inhibiting miR-494-3p led to elevated TRIM36 expression (Fig. 3E). The results indicate that TRIM36 was a direct downstream target of miR-494-3p.

EPS1-1 limits HCC cell development via the miR-494-3p/TRIM36 axis

The role of TRIM36 in the inhibition of HCC by EPS1-1 was investigated by monitoring TRIM36 levels in HCC cells following EPS1-1 treatment at different concentrations. Both mRNA and protein expression of TRIM36 were significantly increased in cells treated with 100 μg/mL and 200 μg/mL EPS1-1 compared with the 0 μg/mL EPS1-1 control (Fig. 4A). To clarify the relative contributions of TRIM36 and miR-494-3p in EPS1-1-mediated effects on HCC, the cells were transfected with oe-TRIM36, sh-TRIM36, or miR-494-3p mimic+oe-TRIM36 before being treated with 200 μg/mL of EPS1-1. As expected, TRIM36 expression was reduced in the EPS1-1 + sh-TRIM36 group and elevated in the (EPS1-1 + oe-TRIM36) group compared with their non-silencing controls (Fig. 4C). Interestingly, when TRIM36 was cotransfected with miR-494-3p and then stimulated with EPS1-1, TRIM36 expression did not increase compared with the oe-TRIM36 group stimulated with EPS1-1 only (Fig. 4B, C), which supported a finding that TRIM36 was downstream of miR-494-3p in HCC. In addition, as shown in Figure 4D–G, HCC cell proliferation and cyclin D and cyclin E expression were significantly increased and p21 expression and apoptosis were significantly decreased when TRIM36 was silenced in spite of EPS1-1 stimulation. The results were reversed, with decreased proliferation and cyclin expression and increased apoptosis and p21 expression when TRIM36 was overexpressed, but the effects were minimized when miR-494-3p was upregulated despite TRIM36 overexpression (Fig. 4D–G). Collectively, the data demonstrate that EPS1-1 hindered HCC cell proliferation and stimulated cell apoptosis by regulating the miR-494-3p/TRIM36 signaling.

TRIM36 induces ubiquitination of cyclin E

The results suggested that EPS1-1 and miR-494-3p regulate the expression of cyclin E protein in HCC, and the GeneCards database (https://www.genecards.org/) provided information regarding the unique E3 ubiquitin ligase activity of TRIM36. We therefore hypothesized that TRIM36 played a crucial role in cell proliferation, migration, and invasion by regulating the ubiquitination of cyclin E or cyclin D. The results showed that while TRIM36 was unable to ubiquitinate cyclin D, it did induce cyclin E ubiquitination. Overexpression of TRIM36 did not change cyclin E transcription (Fig. 5A), but significantly inhibited its protein expression (Fig. 5B), but that was blunted by treatment with the protease inhibitor MG132 (Fig. 5B), consistent with TRIM36 participation in the post-transcriptional regulation of cyclin E through ubiquitination. Co-immunoprecipitation procedures revealed that cyclin E was not pulled down by IgG treatment, but that anti-TRIM36 antibody managed to immune-precipitate cyclin E. Similarly, when cyclin E was immune-precipitated, TRIM36 expression effectively increased and coprecipitated (Fig. 5C). Analysis of ubiquitination further confirmed that TRIM36 induced ubiquitination of cyclin E (Fig. 5D). The data suggest that TRIM36 inhibited HCC development by binding and inducing the ubiquitination of cyclin E.

EPS1-1 inhibits tumor growth in vivo

To examine the importance of miR-494-3p in the tumor-suppressive activity of EPS1-1 *in vivo*, subcutaneous xenografts in nude mice were evaluated. The experiments revealed that EPS1-1 treatment significantly reduced tumor volume and weight. The inhibitory functions of EPS1-1 were significantly reduced when the miR-494-3p mimic was added to the treatment (Fig. 6A, B). TUNEL assays showed that EPS1-1 treatment substantially promoted tumor cell apoptosis compared with the control. Apoptosis significantly decreased in the EPS1-1treated miR-494-3p mimic group

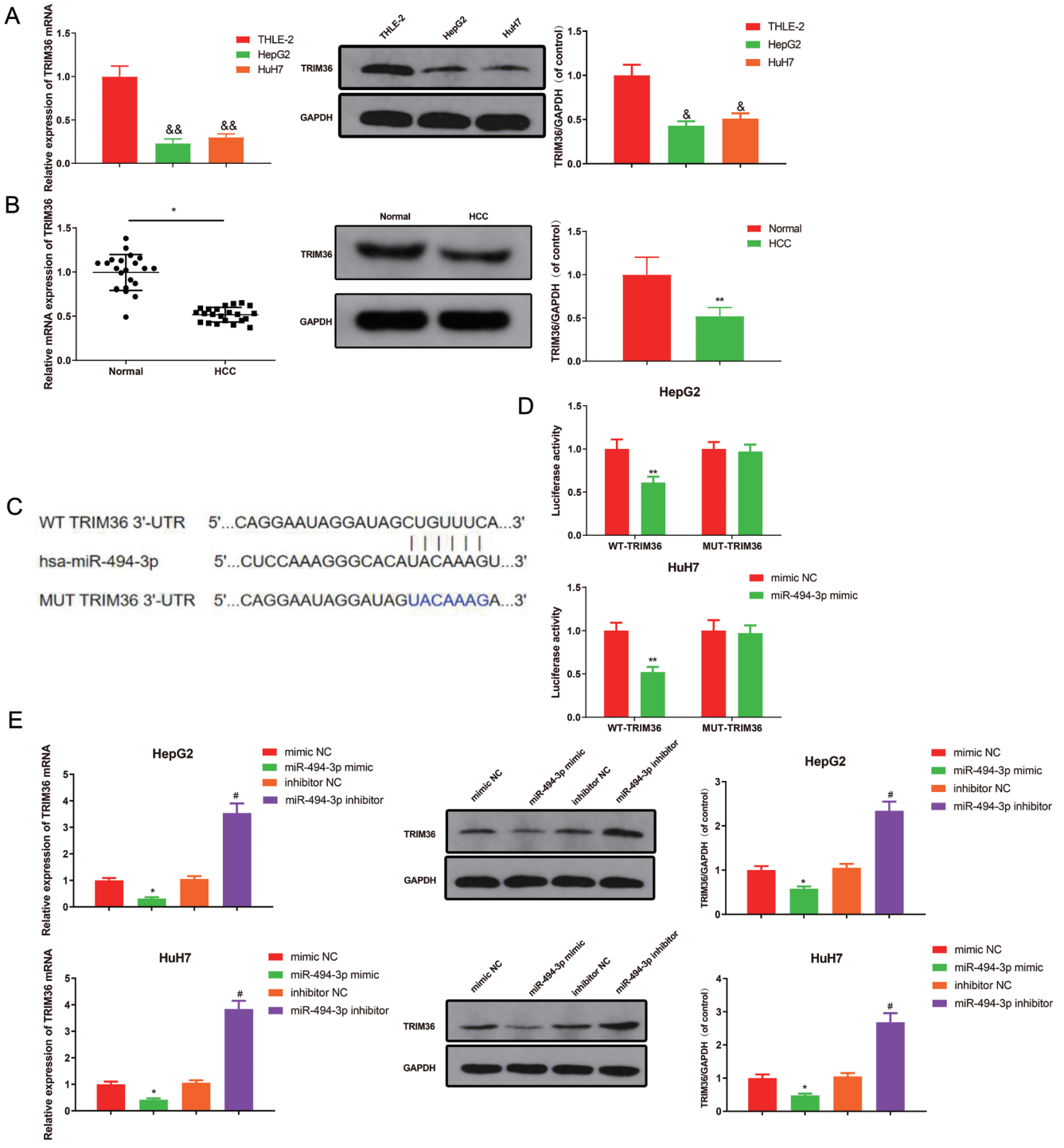

Fig. 3. TRIM36 is a direct target gene of miR-494-3p. qRT-PCR and western blot assays of TRIM36 expression in HCC cells and tissues (A, B). Possible miR-494-3p and TRIM36 binding sites predicated by StarBase (C). Dual luciferase reporter assay of the interaction between miR-494-3p and TRIM36 (D). qRT-PCR and western blot assays of TRIM36 expression in HCC cells in each study group (E). *p<0.05, **p<0.01 vs. mimic NC or normal cells. $^{\&}p$<0.05, $^{\&\&}p$<0.01 vs. THLE-2. $^{\#}p$<0.05 vs. inhibitor NC. Data are means ± standard deviation; independent-sample t-test. HCC, hepatocellular carcinoma.

compared to its control (Fig. 6C). The relationship between miR-494-3p, TRIM36, and the effects of EPS1-1 on the expression of TRIM36 and cyclin E were also evaluated *in vivo*. qRT-PCR and IHC staining confirmed that EPS1-1 treatment upregulated TRIM36 expression and downregulated cyclin E expression (Fig. 6D-E) and that miR-494-3p mimic treatment reduced TRIM36 expression and increased cyclin E expression (Fig. 6D–E). Immunofluorescence double staining found that TRIM36 co-localized with cyclin E in cell nuclei (Fig. 6F). Overall, these results show that EPS1-1 inhib-

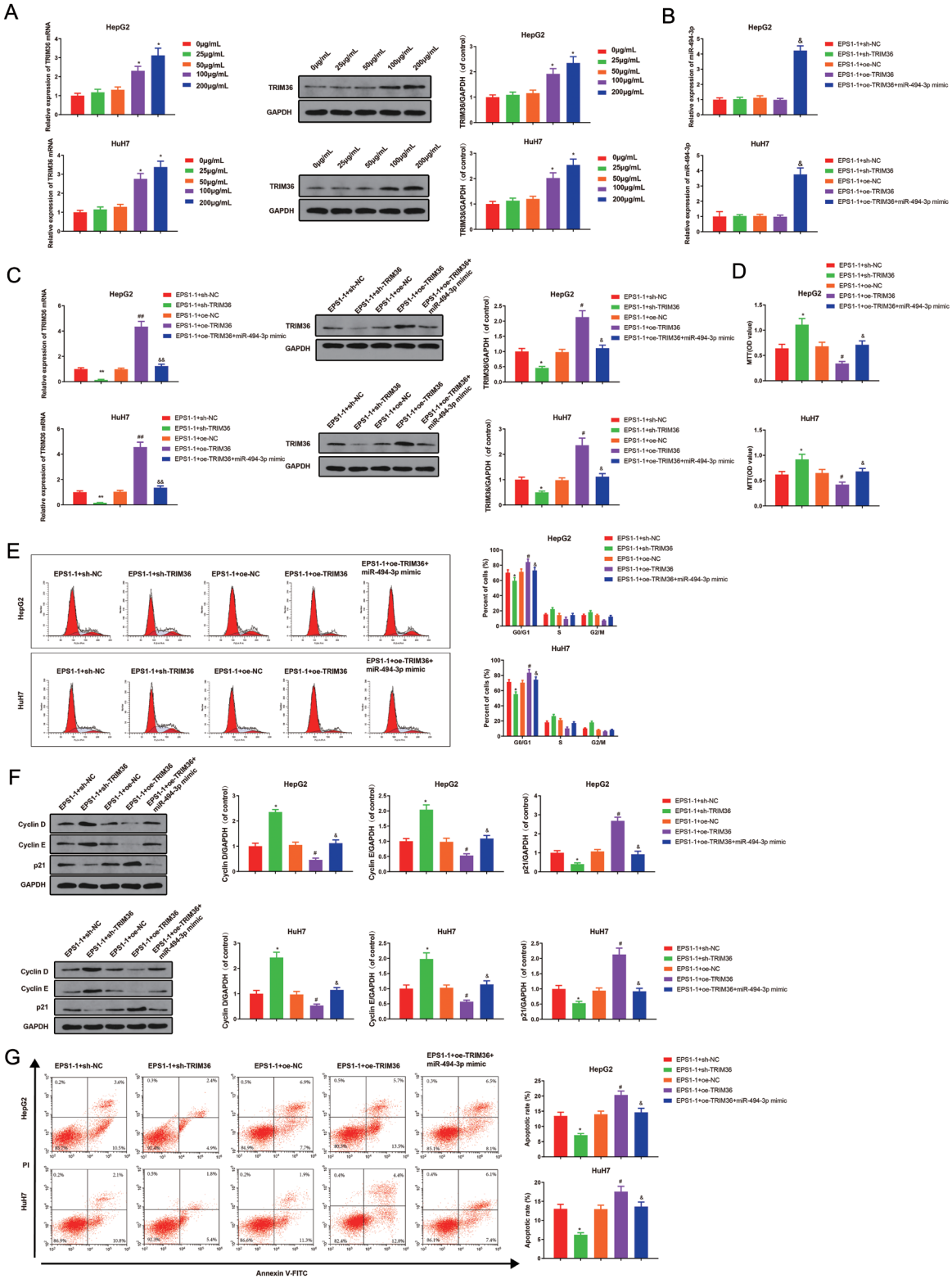

Fig. 4. EPS1-1 affects HCC cell progression via miR-494-3p/TRIM36 axis. qRT-PCR and western blot assays of TRIM36 expression in HCC cells treated with different concentrations of EPS1-1 (A). qRT-PCR assays of miR-494-3p expression (B). Expression of of TRIM36 mRNA and protein (C). Assays of HCC cell proliferation, cell cycle, cell cycle regulatory proteins, and cell apoptosis by MTT (D), FCM (E), Western blot (F), and Annexin V-FITC/PI staining (G), respectively. *p<0.05, **p<0.01 vs. control or EPS1-1 + sh-NC. $^{\#}P$<0.05; $^{\#\#}p$<0.01 vs. EPS1-1 + oe-NC; $^{\&}p$<0.05; $^{\&\&}p$<0.01 vs. EPS1-1 + oe-TRIM36. Data are means ± standard deviation; independent-sample t-test or one-way analysis of variance and Tukey's. Each assay was performed in triplicate. FCM, flow cytometry; HCC, hepatocellular carcinoma; PI, propidium iodide.

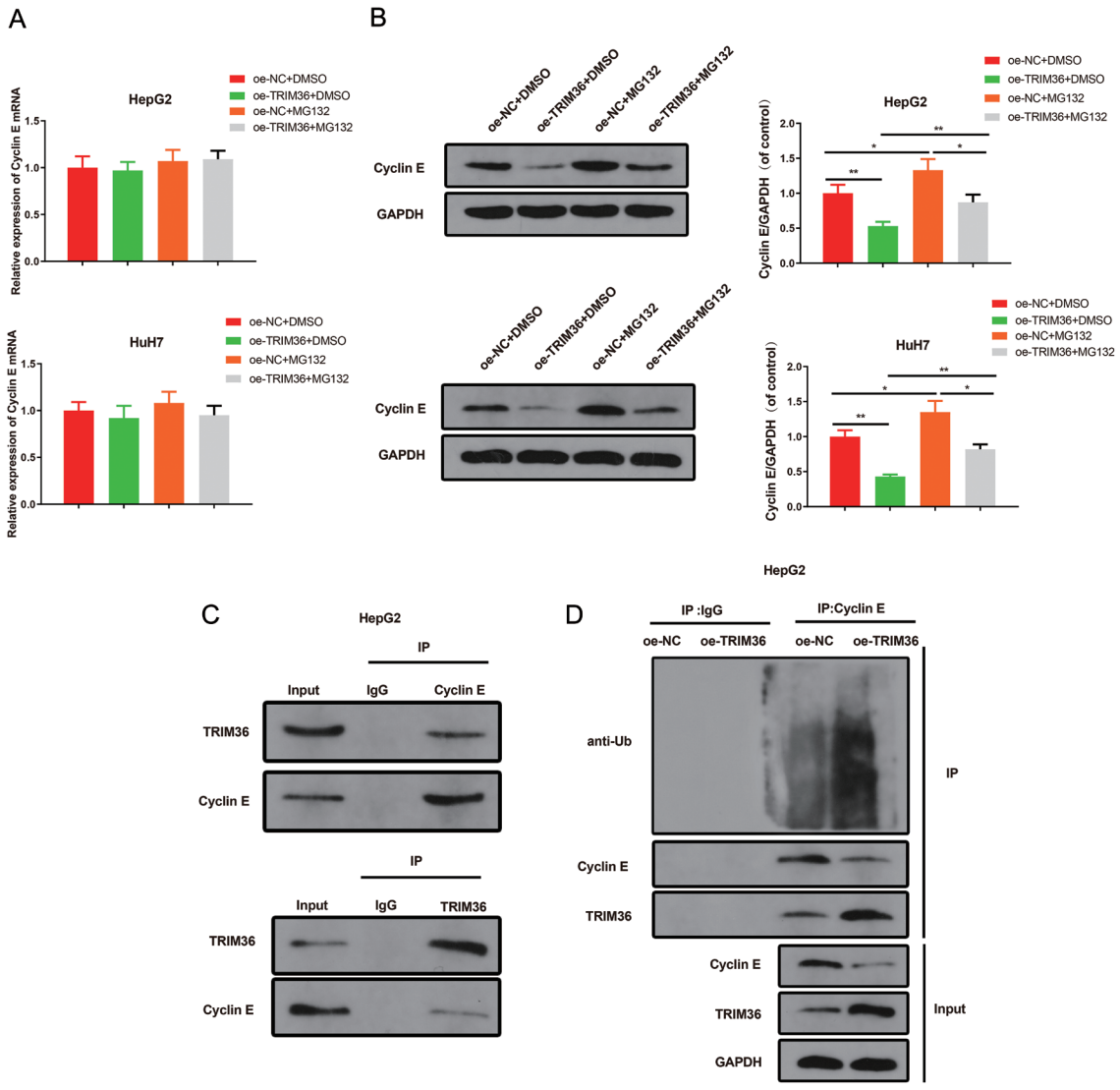

Fig. 5. TRIM36 stimulates ubiquitination of cyclin E. qRT-PCR and Western blot assays of cyclin E mRNA and protein expression (A, B). Co-immunoprecipitation (CO-IP) confirms the interaction between TRIM36 and cyclin E (C). TRIM36 elicits ubiquitination of cyclin E (D). *p<0.05, **p<0.01 vs. oe-NC+DMSO, oe-TRIM36+DMSO, or oe-NC+MG132. Data are means ± standard deviation; independent-samples t-test of one-way analysis of variance and Tukey's test. Each assay was performed in triplicate.

ited HCC development *in vivo* by modulating miR-494-3p/TRIM36 signaling and cyclin E ubiquitination.

Discussion

In this study, we evaluated the effects of EPS1-1 on HCC *in vitro* and *in vivo*. We observed that EPS1-1 treatment inhibited HCC cell progression by downregulating the tumor promoter miR-494-3p to promote TRIM36 expression, which in turn induced ubiquitination of cyclin E. Previous studies have shown that EPS1-1 has antitumor activity *in vitro* and *in vivo*[9,23] and was reported to be a tumor suppressor in HCC,[15] but causative relationships have not been elucidated yet. This study investigated the *in vitro* and *in vivo* inhibition of HCC cell and tumor growth of HCC by EPS1-1 polysaccharide extracted from *R. nigrum*. EPS1-1, at concentrations of 25–200 μg/mL decreased HCC cell proliferation in a time- and dose-dependent manner. Cell cycle suppression is recognized as a potential target in cancer therapy,[24] and in this study, EPS1-1 treatment induced G0/G1 phase arrest in HCC cells. Cell cycle progression is dependent on CDK, arrested by CDK inhibitors, and activated by cyclin binding.[25] EPS1-1 reduced the expression of the cell cycle regulatory proteins cyclin D and cyclin E expression and it increased the expression of p21, a CDK inhibitor, (p21) in a dose-dependent manner, indicating potent inhibitory effects of EPS1-1 on HCC cell proliferation. Promotion of cell apoptosis is an important mechanism of action of anticancer drugs,[26] and EPS1-1 at 100 and 200 μg/mL significantly promoted the apoptosis of HCC cells. Our findings demonstrate the anti-proliferative and pro-apoptotic effects of EPS1-1 in HCC cells, which is not only in line with earlier studies but a further confirmation of the effects of EPS1-1 on cancer cell progression. Nonetheless, the working molecular mechanism of EPS1-1 has not been previously described.

In recent years, miRNAs have been shown to play sig-

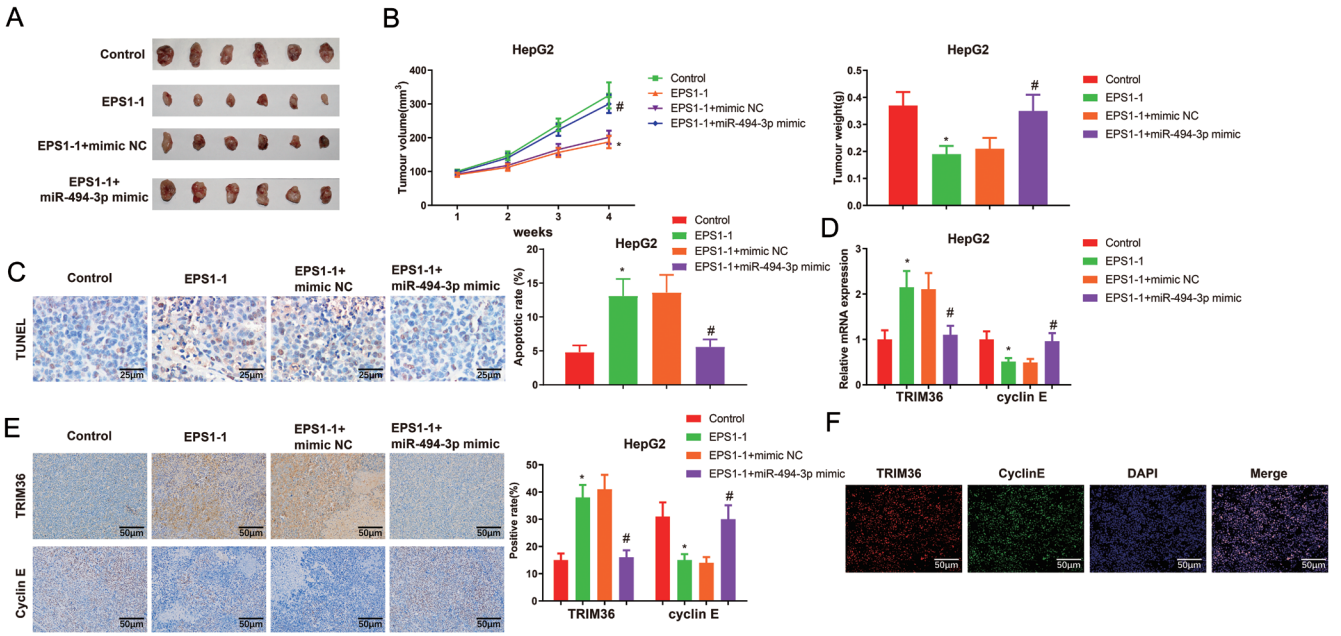

Fig. 6. EPS1-1 suppresses tumor growth *in vivo*. Photographs of subcutaneous xenograft tumor (A). Tumor volume and weight in each group (B). TUNEL staining assay of apoptosis (C). qRT-PCR and IHC assays of TRIM36 and cyclin E expression in tumor tissues of nude mice (D, E). Immunofluorescence assays show the location of TRIM36 and cyclin E (F). n = 6, *p<0.05 vs. control; $^{\#}p$<0.05 vs. EPS1-1 + mimic NC. Data are means ± standard deviation; independent-samples t-test. IHC, immunohistochemistry.

nificant roles in modulating the progression of several types of cancers, including HCC.[27] Previous studies indicated that miR-494-3p is upregulated in HCC,[22,28] and suggested it is a tumor promoter in HCC. Herein, we demonstrated that miR-494-3p was a key player in EPS1-1-mediated inhibition of HCC. We also showed that miR-494-3p was overexpressed in HCC cells and significantly suppressed following EPS1-1 treatment (100 μg/mL and 200 μg/mL). Moreover, in the presence of EPS1-1, miR-494-3p overexpression significantly promoted proliferation and cyclin D/E expression in HCC cells while it decreased p21 expression, the percentage of cells in the G0/G1 phase, and apoptosis. Taken together, the data reveal that EPS1-1 suppressed HCC proliferation and boosted cell apoptosis via inhibiting miR-494-3p expression.

miRNAs directly bind to the 3′-UTR of target mRNAs and then downregulate expression of the corresponding gene.[29,30] TRIM36 a TRIM family member, was identified as a target of miR-320a.[31] Previously, TRIM36 downregulation was reported in gastric and prostate cancer cells and tissues, but its expression in HCC has not been reported.[32,33] We found that TRIM36 was weakly expressed in HCC and it had a binding site for miR-494-3p. Overexpression of miR-494-3p in HCC suppressed TRIM36 expression and inhibition of miR-494-3 enhanced TRIM36 expression. Increased TRIM36 expression has been shown to indicate a favorable prognosis, and TRIM36 is a tumor suppressor in prostate cancer by inhibiting cell proliferation and stimulating apoptosis.[32] This background prompted us to explore the role of TRIM36 in the inhibition of EPS1-1 in HCC. TRIM36 levels were upregulated by EPS1-1 treatment. Cell proliferation was enhanced, and cell apoptosis was decreased, by TRIM36 inhibition and EPS1-1 treatment. The presence of both EPS1-1 and TRIM36 overexpression effectively blunted the progression of HCC cells. Moreover, miR-494-3p overexpression partially counteracted the synergic effects of EPS1-1 and TRIM36 on suppressing HCC. The data support EPS1-1 suppression of HCC cell development via a miR-494-3p/TRIM36 axis. The TRIM protein family includes E3 ubiquitin ligases with activity related to a broad range of biological and pathological processes.[34] Our data demonstrated that TRIM36 has unique E3 ubiquitin ligase activity and TRIM36 overexpression induced the ubiquitination of cyclin E in HCC. Additionally, *in vivo* animal experiments revealed that administration of EPS1-1 repressed tumor growth in nude mice by regulating miR-494-3p/TRIM36 axis and ubiquitination of cyclin E. In addition to TRIM36, miR-494-3p has been reported to promote HCC metastasis by targeting PTEN,[22] and the regulatory activity was reported in non-small cell lung cancer and glioma in which miR-494-3p was sponged by the long noncoding RNA WT1-AS1.[21,35,36] In-depth studies are needed to elucidate the impact of the interactions between miR-494-3p and other known HCC targets, which would facilitate the development of miRNA-based treatment of HCC.

Conclusion

In summary, our study describes a working molecular mechanism for EPS1-1 inhibition of proliferation and survival of HCC *in vitro* and *in vivo*. The inhibitory effects of EPS1-1 were achieved through downregulation of miR-494-3p expression and upregulation of TRIM36-mediated ubiquitination of cyclin E, ultimately regulating the progression of HCC. HCC treatments that include EPS1-1 may be useful and warrant further study.

Funding

None to declare.

Conflict of interest

The authors have no conflict of interests related to this pub-

lication.

Author contributions

Study design (HY, PR), performance of experiments (HY, XM), analysis and interpretation of data (HY, ZM, ZH), manuscript writing (HY, XM), critical revision of the manuscript (PR, XM), technical or material support (PR).

Ethical statement

All procedures involving humans were performed with the approval of the ethics committee of the Third Xiangya Hospital of Central South University and the informed consent of participants or their relatives.

Data sharing statement

All data are accessible upon reasonable request to correspond author.

References

[1] Jemal A, Bray F, Center MM, Ferlay J, Ward E, Forman D. Global cancer statistics. CA Cancer J Clin 2011;61(2):69–90. doi:10.3322/caac.20107, PMID:21296855.

[2] Lin YH, Wu MH, Huang YH, Yeh CT, Cheng ML, Chi HC, *et al*. Taurine up-regulated gene 1 functions as a master regulator to coordinate glycolysis and metastasis in hepatocellular carcinoma. Hepatology 2018;67(1):188–203. doi:10.1002/hep.29462, PMID:28802060.

[3] Uchino K, Tateishi R, Shiina S, Kanda M, Masuzaki R, Kondo Y, *et al*. Hepatocellular carcinoma with extrahepatic metastasis: clinical features and prognostic factors. Cancer 2011;117(19):4475–4483. doi:10.1002/cncr.25960, PMID:21437884.

[4] Uka K, Aikata H, Takaki S, Shirakawa H, Jeong SC, Yamashina K, *et al*. Clinical features and prognosis of patients with extrahepatic metastases from hepatocellular carcinoma. World J Gastroenterol 2007;13(3):414–420. doi:10.3748/wjg.v13.i3.414, PMID:17230611.

[5] Kokudo T, Hasegawa K, Shirata C, Tanimoto M, Ishizawa T, Kaneko J, *et al*. Assessment of Preoperative Liver Function for Surgical Decision Making in Patients with Hepatocellular Carcinoma. Liver Cancer 2019;8(6):447–456. doi:10.1159/000501368, PMID:31799202.

[6] Dong Z, Feng L, Hao Y, Chen M, Gao M, Chao Y, *et al*. Synthesis of Hollow Biomineralized CaCO3-Polydopamine Nanoparticles for Multimodal Imaging-Guided Cancer Photodynamic Therapy with Reduced Skin Photosensitivity. J Am Chem Soc 2018;140(6):2165–2178. doi:10.1021/jacs.7b11036, PMID:29376345.

[7] Pan TJ, Li LX, Zhang JW, Yang ZS, Shi DM, Yang YK, *et al*. Antimetastatic Effect of Fucoidan-Sargassum against Liver Cancer Cell Invadopodia Formation via Targeting Integrin αVβ3 and Mediating αVβ3/Src/E2F1 Signaling. J Cancer 2019;10(20):4777–4792. doi:10.7150/jca.26740, PMID:31598149.

[8] Hussain SS, Kumar AP, Ghosh R. Food-based natural products for cancer management: Is the whole greater than the sum of the parts? Semin Cancer Biol 2016;40-41:233–246. doi:10.1016/j.semcancer.2016.06.002, PMID:27397504.

[9] Yu W, Chen G, Zhang P, Chen K. Purification, partial characterization and antitumor effect of an exopolysaccharide from Rhizopus nigricans. Int J Biol Macromol 2016;82:299–307. doi:10.1016/j.ijbiomac.2015.10.005, PMID:26449531.

[10] Yu Z, Kong M, Zhang P, Sun Q, Chen K. Immune-enhancing activity of extracellular polysaccharides isolated from Rhizopus nigricans. Carbohydr Polym 2016;148:318–325. doi:10.1016/j.carbpol.2016.04.068, PMID:27185145.

[11] Bouattour M, Mehta N, He AR, Cohen EI, Nault JC. Systemic Treatment for Advanced Hepatocellular Carcinoma. Liver Cancer 2019;8(5):341–358. doi:10.1159/000496439, PMID:31768344.

[12] Feng B, Zhu Y, Sun C, Su Z, Tang L, Li C, *et al*. Basil polysaccharide inhibits its hypoxia-induced hepatocellular carcinoma metastasis and progression through suppression of HIF-1α-mediated epithelial-mesenchymal transition. Int J Biol Macromol 2019;137:32–44. doi:10.1016/j.ijbiomac.2019.06.189, PMID:31252022.

[13] Song G, Lu Y, Yu Z, Xu L, Liu J, Chen K, *et al*. The inhibitory effect of polysaccharide from Rhizopus nigricans on colitis-associated colorectal cancer. Biomed Pharmacother 2019;112:108593. doi:10.1016/j.biopha.2019.01.054, PMID:30784912.

[14] Yu Z, Sun Q, Liu J, Zhang X, Song G, Wang G, *et al*. Polysaccharide from Rhizopus nigricans inhibits the invasion and metastasis of colorectal cancer. Biomed Pharmacother 2018;103:738–745. doi:10.1016/j.biopha.2018.04.093, PMID:29684852.

[15] Chu G, Miao Y, Huang K, Song H, Liu L. Role and Mechanism of Rhizopus Nigrum Polysaccharide EPS1-1 as Pharmaceutical for Therapy of Hepatocellular Carcinoma. Front Bioeng Biotechnol 2020;8:509. doi:10.3389/fbioe.2020.00509, PMID:32582655.

[16] Wilk G, Braun R. Integrative analysis reveals disrupted pathways regulated by microRNAs in cancer. Nucleic Acids Res 2018;46(3):1089–1101. doi:10.1093/nar/gkx1250, PMID:29294105.

[17] Li H, Zhao X, Shan H, Liang H. MicroRNAs in idiopathic pulmonary fibrosis: involvement in pathogenesis and potential use in diagnosis and therapeutics. Acta Pharm Sin B 2016;6(6):531–539. doi:10.1016/j.apsb.2016.06.010, PMID:27818919.

[18] Toffanin S, Hoshida Y, Lachenmayer A, Villanueva A, Cabellos L, Minguez B, *et al*. MicroRNA-based classification of hepatocellular carcinoma and oncogenic role of miR-517a. Gastroenterology 2011;140(5):1618–1628.e16. doi:10.1053/j.gastro.2011.02.009, PMID:21324318.

[19] Hou J, Lin L, Zhou W, Wang Z, Ding G, Dong Q, *et al*. Identification of miRNomes in human liver and hepatocellular carcinoma reveals miR-199a/b-3p as therapeutic target for hepatocellular carcinoma. Cancer Cell 2011;19(2):232–243. doi:10.1016/j.ccr.2011.01.001, PMID:21316602.

[20] Huang N, Lin J, Ruan J, Su N, Qing R, Liu F, *et al*. MiR-219-5p inhibits hepatocellular carcinoma cell proliferation by targeting glypican-3. FEBS Lett 2012;586(6):884–891. doi:10.1016/j.febslet.2012.02.017, PMID:22449976.

[21] Li XT, Wang HZ, Wu ZW, Yang TQ, Zhao ZH, Chen GL, *et al*. miR-494-3p Regulates Cellular Proliferation, Invasion, Migration, and Apoptosis by PTEN/AKT Signaling in Human Glioblastoma Cells. Cell Mol Neurobiol 2015;35(5):679–687. doi:10.1007/s10571-015-0163-0, PMID:25662849.

[22] Lin H, Huang ZP, Liu J, Qiu Y, Tao YP, Wang MC, *et al*. MiR-494-3p promotes PI3K/AKT pathway hyperactivation and human hepatocellular carcinoma progression by targeting PTEN. Sci Rep 2018;8(1):10461. doi:10.1038/s41598-018-28519-2, PMID:29992971.

[23] Cao J, Hou D, Lu J, Zhu L, Zhang P, Zhou N, *et al*. Anti-tumor activity of exopolysaccharide from Rhizopus nigricans Ehrenb on S180 tumor-bearing mice. Bioorg Med Chem Lett 2016;26(8):2098–2104. doi:10.1016/j.bmcl.2016.02.012, PMID:26951752.

[24] Siddiqui IA, Bharali DJ, Nihal M, Adhami VM, Khan N, Chamcheu JC, *et al*. Excellent anti-proliferative and pro-apoptotic effects of (-)-epigallocatechin-3-gallate encapsulated in chitosan nanoparticles on human melanoma cell growth both in vitro and in vivo. Nanomedicine 2014;10(8):1619–1626. doi:10.1016/j.nano.2014.05.007, PMID:24965756.

[25] Komata T, Kanzawa T, Takeuchi H, Germano IM, Schreiber M, Kondo Y, *et al*. Antitumour effect of cyclin-dependent kinase inhibitors (p16(INK4A), p18(INK4C), p19(INK4D), p21(WAF1/CIP1) and p27(KIP1)) on malignant glioma cells. Br J Cancer 2003;88(8):1277–1280. doi:10.1038/sj.bjc.6600862, PMID:12698196.

[26] Sverchinsky DV, Nikotina AD, Komarova EY, Mikhaylova ER, Aksenov ND, Lazarev VF, *et al*. Etoposide-Induced Apoptosis in Cancer Cells Can Be Reinforced by an Uncoupled Link between Hsp70 and Caspase-3. Int J Mol Sci 2018;19(9):2519. doi:10.3390/ijms19092519, PMID:30149619.

[27] Zhou J, Yu L, Gao X, Hu J, Wang J, Dai Z, *et al*. Plasma microRNA panel to diagnose hepatitis B virus-related hepatocellular carcinoma. J Clin Oncol 2011;29(36):4781–4788. doi:10.1200/JCO.2011.38.2697, PMID:22105822.

[28] Pollutri D, Patrizi C, Marinelli S, Giovannini C, Trombetta E, Giannone FA, *et al*. The epigenetically regulated miR-494 associates with stem-cell phenotype and induces sorafenib resistance in hepatocellular carcinoma. Cell Death Dis 2018;9(1):4. doi:10.1038/s41419-017-0076-6, PMID:29305580.

[29] Jaiswal A, Reddy SS, Maurya M, Maurya P, Barthwal MK. MicroRNA-99a mimics inhibit M1 macrophage phenotype and adipose tissue inflammation by targeting TNFα. Cell Mol Immunol 2019;16(5):495–507. doi:10.1038/s41423-018-0038-7, PMID:29849090.

[30] O'Neill LA, Sheedy FJ, McCoy CE. MicroRNAs: the fine-tuners of Toll-like receptor signalling. Nat Rev Immunol 2011;11(3):163–175. doi:10.1038/nri2957, PMID:21331081.

[31] Pandey A, Sahu AR, Wani SA, Saxena S, Kanchan S, Sah V, *et al*. Modulation of Host miRNAs Transcriptome in Lung and Spleen of Peste des Petits Ruminants Virus Infected Sheep and Goats. Front Microbiol 2017;8:1146. doi:10.3389/fmicb.2017.01146, PMID:28694795.

[32] Kimura N, Yamada Y, Takayama KI, Fujimura T, Takahashi S, Kume H, *et al*. Androgen-responsive tripartite motif 36 enhances tumor-suppressive effect by regulating apoptosis-related pathway in prostate cancer. Cancer Sci 2018;109(12):3840–3852. doi:10.1111/cas.13803, PMID:30238687.

[33] Man Z, Chen T, Zhu Z, Zhang H, Ao L, Xi L, *et al*. High expression of TRIM36 is associated with radiosensitivity in gastric cancer. Oncol Lett 2019;17(5):4401–4408. doi:10.3892/ol.2019.10122, PMID:30944633.

[34] Tan J, Shen J, Zhu H, Gong Y, Zhu H, Li J, *et al*. miR-378a-3p inhibits ischemia/reperfusion-induced apoptosis in H9C2 cardiomyocytes by targeting TRIM55 via the DUSP1-JNK1/2 signaling pathway. Aging (Albany NY) 2020;12(10):8939–8952. doi:10.18632/aging.103106, PMID:32463795.

[35] Wu C, Yang J, Li R, Lin X, Wu J, Wu J. LncRNA WT1-AS/miR-494-3p Regulates Cell Proliferation, Apoptosis, Migration and Invasion via PTEN/PI3K/AKT Signaling Pathway in Non-Small Cell Lung Cancer. Onco Targets Ther 2021;14:891–904. doi:10.2147/OTT.S278233, PMID:33603394.

[36] Qiu G, Tong W, Jiang C, Xie Q, Zou J, Luo C, *et al*. Long Noncoding RNA WT1-AS Inhibit Cell Malignancy via miR-494-3p in Glioma. Technol Cancer Res Treat 2020;19:1533033820919759. doi:10.1177/1533033820919759, PMID:32419643.